



# Study of the microstructures and mineralogical phases in the fault gouge and their relationship with the fault seismicity, a case study of the Astaneh fault

Mohammadreza Hajianezhad <sup>1\*</sup>, Behnam Rahimi <sup>2</sup>

<sup>1</sup> Institute of Geophysics, University of Tehran, Iran

<sup>2</sup> Department of geology, Faculty of science, Ferdowsi University of Mashhad, Iran

Received 07 June 2023, Revised: 18 December 2023, Accepted: 01 January 2024

© University of Tehran

## Abstract

The Astaneh Fault is one of the active and seismic faults in the Shahroud sinistral fault system. Fault gouges can be seen in a completely pristine and unchanged form in the portions of this fault that have affected the carbonate rocks. Fault gouges are the direct product of lithology and are formed as a result of the fault slip from the host rocks. Studying these rocks for type, composition, mineralogical phases and structure can provide results on how the fault slip and gouge process occurs. The result of a seismic slip in faults, and especially in gouges, are different types of deformations, such as mineralogical and compositional deformations, depending on the conditions of their formation. From this deformation model, we can mention the thermal decomposition of calcite and dolomite, as well as the presence of siderite in gouges. In this article, by studying the combined [aggregated] microstructures in the Astaneh fault gouge, their relationship with seismic slip has been investigated. According to previous research, the Astaneh Fault is certainly a seismic fault. The presence of the resulting thermal decomposition of calcite and dolomite (calcium and magnesium oxide or periclase) and the welding of particles due to heat may be the key to seismic slip in this fault.

**Keywords:** Active Fault, Fault Gouge, Thermal Decomposition, Seismic Slip

## Introduction

A significant variety of different fault rock types is observed in many areas with natural and pristine fault zones (Sibson 1977; Imber et al. 2001; Watts et al. 2007). This variety of rock faults in terms of type and number shows the balance of a large number of structural and metamorphism processes and also the interaction between these processes that occur at different times and at different depths and under different conditions in the crust (Knipe 1989). Fault rock type has a significant impact on the state of permeability, strength, and frictional stability of fault zones, and has important implications for fluid flow-related seismicity and mineralization (Scholz 2002, Caine et al. 1996, Jefferies et al 2006, Moore & Rymer 2007, Colletini et al 2009a, Tullis et al 2007; Smith et al. 2013).

Gouges are fine-grained rock faults that should be considered as a direct lithological product of fault activity. These fault rocks are formed by relatively complex physical and chemical processes associated with the low-level metamorphism that accompanies fault slip (Bos et al., 2000). Therefore, the microstructures in the gouge contain information about slip and fault behavior as well as the nature of the physical and chemical environment along the fault zone

---

\* Corresponding author e-mail: m.hajian58@gmail.com

during faulting (Reinen, 2000; Zhang et al., 2002; Yuan et al., 2013).

Recent investigations in various locations around the world have shown that deformation in the brittle upper crust occurs first in larger areas of fracture and cataclasite. Then in relatively large areas thin layers (2 to 3 m) are concentrated from fine-grained and foliated fault gouge (Cladouhos 1999; Cowan et al. 2003; Hayman et al. 2004).

In recent years, the study of carbonate fault rocks and gouges has been significantly advanced and systematized due to their importance in the hydrocarbon industry (Burkhardt, 1993; De Bresser & Spier, 1993; Hadizadeh, 1994; Newman & Mitra, 1994; Babaei et al., 1995; Kennedy & Logan, 1997; Salvini et al., 1999; Graham et al., 2003; Kim et al., 2003; Liana-Funz et al. 2005; Storti et al., 2003; Augusta et al., 2007; Tondi, 2007). Recent studies such as the evolution of grain shape during fault slip, fault core (gouge) permeability, and examination of some seismic indicators obtained in laboratory simulated faults have greatly enhanced our understanding of the mechanical and hydraulic behavior of carbonate fault rocks (Ghisetti et al., 2001; Augusta & Kirchner, 2003; Micarelli et al., 2006; Augusta et al., 2007; Storti et al., 2003; Han et al., 2007a, Billi and Di Toro, 2008). Han et al. (2010) conducted an experiment to simulate seismic slip rates in Carrara marble. They concluded that seismic processes and associated indicators should be studied at the micro-scale. Unfortunately, the microstructure of low-temperature, low-pressure carbonate rocks has not been adequately studied and published microscopic images of these rocks are rare (Pieri et al., 2001a; Barnhoorn, et al., 2004, Friel & Morris, 2008; Moret & Woodcock, 2008). This lack of knowledge certainly hinders understanding of the processes responsible for the formation of carbonate fault cores (gouges) and understanding of the frictional and hydraulic behavior of these structures.

The Astaneh fault is a seismic fault whose last seismic activity is related to the present epoch (Holocen; Hollingsworth et al. 2010, Nemati et al. 2012, Shokri et al. 2008) with the current strike-slip mechanism and is located to the south of eastern Alborz in Iran. This fault exhibits an unweathered and prominent calcareous fault zone and fault gouge that is completely pristine and untouched due to the conditions prevailing there. Studying it, one can certainly see the diversity in the performance of multiple deformation mechanisms. Some of these mechanisms reflect progressive deformation over time. While others also point to the nearly simultaneous occurrence of different processes in the fault zone. That they determine how variable yet largely simultaneous deformation mechanisms can affect slip behavior along such faults.

In this study, we describe, using experiments and images, the mineralogical, textural, and structural phases of the upper crustal fault gouges found along the Astaneh Fault. Some of the phases and minerals in the gouge show deformation and fault strength weakening at the onset of an earthquake, such as carbon, while others show only unstable deformation from one mode to another, such as the transformation of calcite into calcium oxide or lime. Among the previous works in this field can refer to Collettini & Holdsworth 2004; Smith et al. 2008; Collettini et al. 2009 a, b noted. Investigations of micro- and nanostructures produced by earthquakes are the subject of much recent research in the field of earthquakes. In many of these studies, the geology related to earthquakes in general is examined from different aspects of earth science, while in many others only specific cases of it are discussed. Results obtained by combining other data are used to identify the source and location of past events and, in some cases, future seismicity and earthquake generation. Although no clear relationship between fault microstructures and seismic activity intensity has been reported so far, some concepts and relationships can be discovered by observing the gouge microstructures of active faults and comparing them to surface-fractured active seismic faults.

In this study, an attempt was made to describe the quantitative and qualitative condition of the existing gouge. Next, based on XRF analysis and SEM images, the nature of the phase changes and their origin and their relationship to past seismic events and the existing structures in the gouge should be investigated. Considering the frictional heat resulting from seismic

activity, some structures and changes can be related to this item in fault rocks. In this study, the thermal decomposition of carbonates and welding of particles due to heat were detected as the result of this in the Astaneh fault.

### **A description of the geological and seismic characteristics of the Astaneh fault**

The Shahroud fault system includes multiple left lateral moving faults in eastern Alborz (Figure 1). The Astaneh Fault lies in the western portion of the sinistral -Shahroud Fault System trending northeast-southwest. This fault is located in the beginning of the eastern Alborz Mountains from the south to the north or (in some writings at the end of central Alborz). This fault was first introduced by Berberian (1984) in the west of Astaneh village as two parallel faults in the form of a left-stepping en echelon with a cut in Quaternary sediments more than 75 km long. He explained that the mechanism of this fault is provided with a straight slip component. Rahimi (2002), Jackson et al. (2002), Nazari (2006), Hollingsworth (2008) and Hollingsworth et al. (2010) also considered it to be a left lateral sliding mechanism.

All field and microstructure observations presented in this study are from the outcrop of the Astaneh fault in carbonate rocks north of Astaneh village (Figure 1). At this point, the fault zone is well exposed at a distance of several hundred meters both in length and in width. This provides an opportunity to evaluate the geometry of the fault zone, the distribution of fault rocks, and the influence of smaller minor faults in the hanging wall and footwall. Elsewhere along the Astaneh fault, where the fault is well exposed (Fig. 1), the authors' field studies show that the fault rocks are often overlain by Quaternary sediments. These issues make interpretation of the rock fault sequence and further investigation difficult or even impossible in this areas.

The Soltan Meydan river flow is located parallels to the Astaneh fault zone 25 km northwest of Damghan town. Hollingsworth (2008) assumes a length of this fault more than one hundred kilometers and places the earthquake rupture on December 22, 856 AD in the Astaneh Valley (In addition, Nemati et al. 2012 and Shokri et al. 2008 also agree that seismic slip in the Astaneh fault caused the great 7.9 magnitude earthquake of December 22, 856). He (Hollingsworth) introduces a pull-apart basin that has been formed by left-lateral slip on the Astaneh fault and he estimates the cumulative horizontal displacement of this fault at 30 kilometers. Geologically, this fault lies between Jurassic dolomite and limestone deposits (Lar Formation) and young river alluvium on the north side of the fault (hanging wall) and Jurassic shale and sandstone and massive Triassic dolomite on the south side of the fault (foot wall). This fault over most of its length together with its branches, forms a relatively wide fault zone, at least in two more or less parallel fault lines at a distance of 15 to 500 meters. Along which there is a valley (Soltan Meydan) with significant coverage of Quaternary deposits (Figure 1). Therefore, the presented observations on the fault rocks alone do not allow to conclusively assert that the Astaneh fault is an active structure and to prove this, other evidence is needed.

A large part of the Astaneh fault between the villages of Astaneh and Foulad Mahalle has a trend of N55E, and there it continues with the same trend to the north of Shahmirzad. Of course, in the meantime, its branches have different trends. Among these branches, there is a branch that extends in an east-west direction.

One of the most important and best evidence and criteria for Quaternary strike-slip faults in fault zones is displacement and deviation along waterways (Arzhannikov et al. 2011). Due to the mountainous nature and extreme topography, many channels and waterways have formed along the Astaneh Fault. Of course, the most important river which is the main river in the region is called the Soltan Maydan and it comes from the east of the Fulad Mahalle neighborhood east-northeast along the same fault that runs along the fault zone, and another example is towards the Qaliche- valley from the northeast. It is moving towards the southwest, but the subchannels cut the entire width of the fault zone and provide very useful information

on how the fault moved in the Quaternary. These waterways have a northwest-southeast direction or vice versa and traverse the width of the Astaneh Fault Zone and for this reason, they show the offset and movement of the fault well.

One of this offset can be observed about ten kilometers southwest of Astaneh Village. This is one of the clearest geomorphological offsets associated with the Quaternary at the eastern end of the Soltan Maydan (Astaneh in some texts) river (Figure 2). All these evidences show that this fault had movement and active in the Quaternary. In addition, many researchers have worked on the seismicity of this fault (Shokri et al. 2008, Nemati et al. 2012, Hollingworth et al. 2010) and all acknowledge that the Qomes earthquake of December 22, 856 AD the magnitude of 7.9 MW was created by slipping the Astaneh Fault. Some others believe the number of historic earthquakes is higher along this fault. In addition, many earthquakes epicenter located along this fault, suggesting that this fault is seismic.

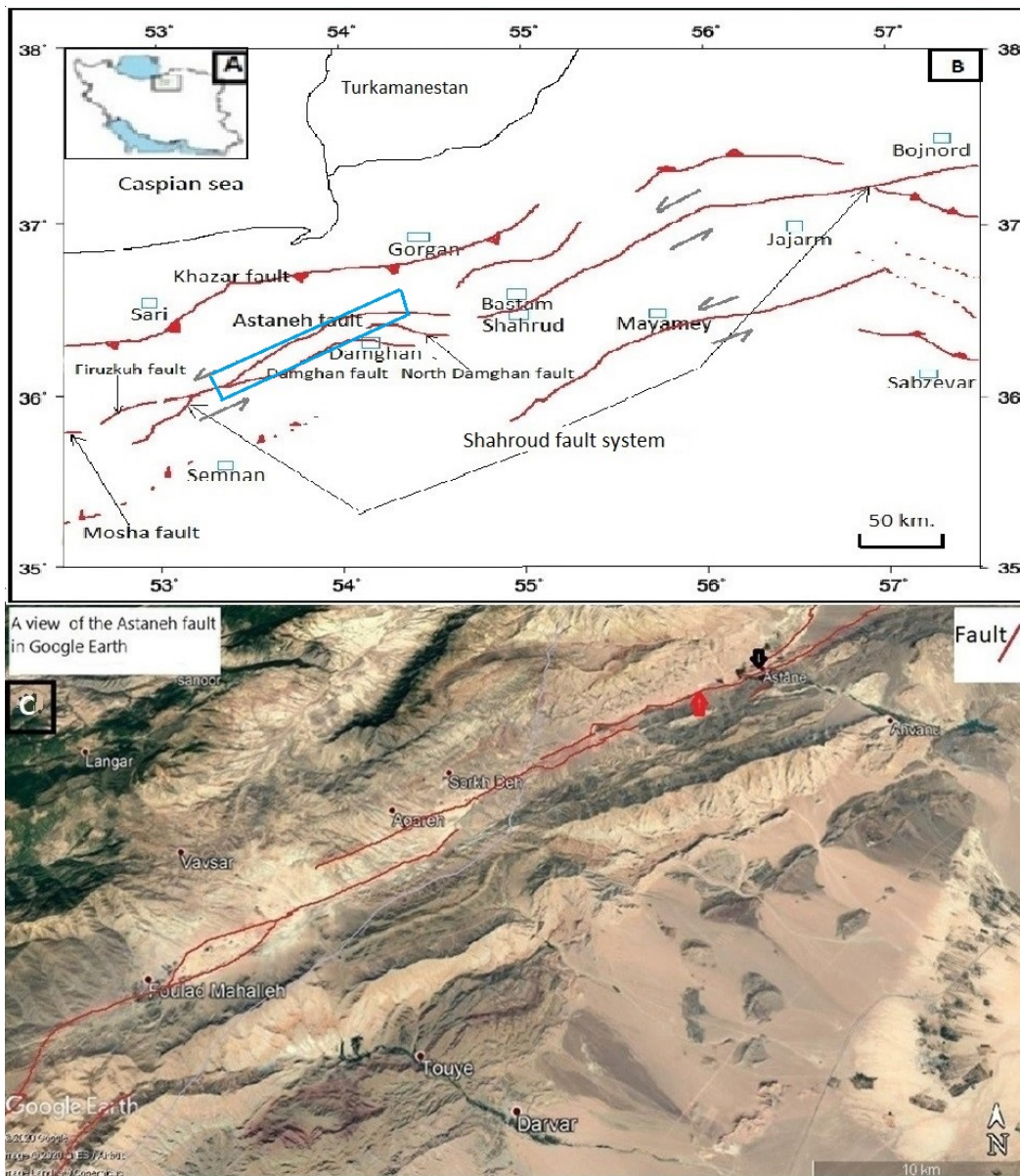


**Figure 1.** A. A view of the studied area and the Shahroud fault system on the map of Iran. B. The faults map and Shahroud fault system in Figure A. The blue rectangle shows the position of the shape of C. (Adapted from Hollingsworth 2007). C. Google Earth image of the Astaneh fault. The red arrow shows

the location of Figure 2 and the black arrow shows the position of figure number 3

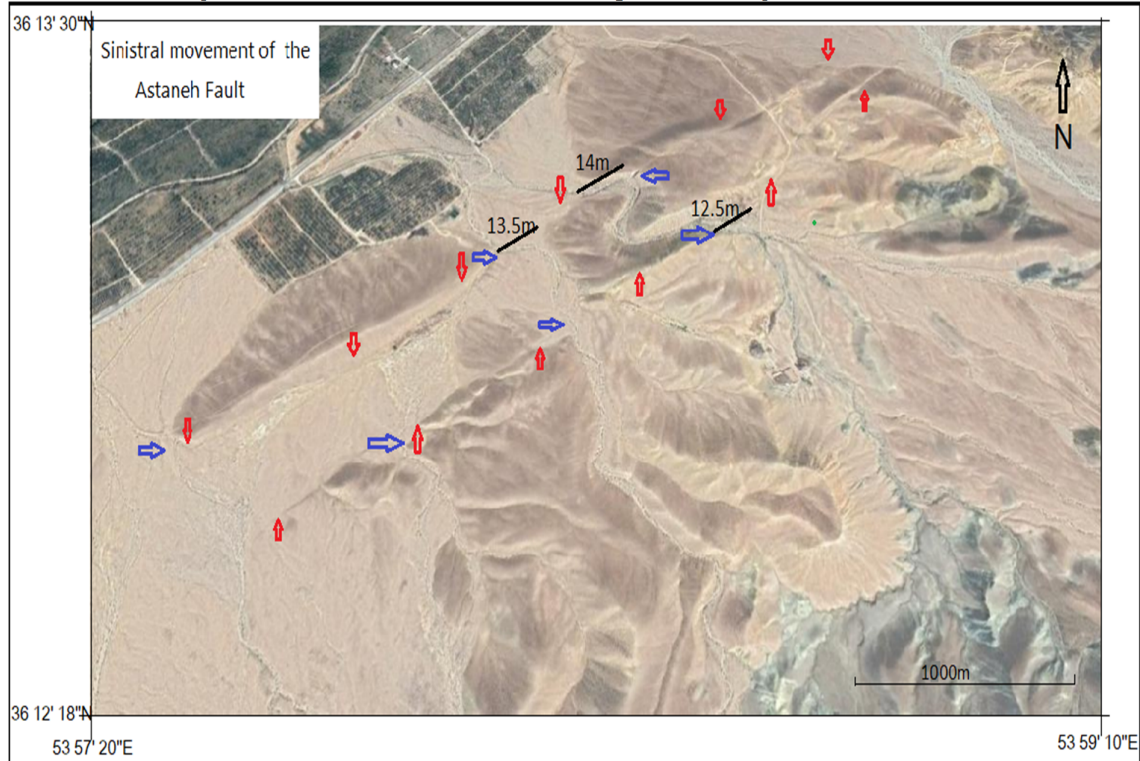


**Figure 2.** A view of two fault lines in Google Earth, the location of which is indicated by the red arrow in Figure 1 and where the left lateral movement through the displacement of streams is clearly visible. The red arrows indicate the two fault lines and the blue arrows indicate where shifting of the streams indicates movement to the left. The black lines and the numbers next to it show the amount of shifts in meters

Geomorphologic evidence along the portion of the fault that cuts through rock units such as Shemshak, Dilichay, and Lar indicates the uplift of the north block and the downfall of the south block. Considering the NW inclination of the fault surface, one can conclude that the ancient (most likely pre-Quaternary) the old movement of the fault is revers mechanism. Regarding the current mechanism of this fault, based on the outcrops north of the village of Astaneh and east of it (Figure 3) and in addition to the cuts in the Quaternary deposits and marls in the Soltan Maydan River and the displacement of seasonal streams with certainty can be called left strike-slip fault (Figure 2). Although the uplift of the northern block and its thrusting onto the southern block is fairly evident, the presence of perfectly horizontal and unweathered slickensides (without weathering and erosion) on both surfaces adjacent to this fault indicates that the final movement of the fault is strike-slip and sinistral (Figure 3).

Rahimi (2002) by studying the surface effect of this fault in different regions, does not consider the Astaneh fault as a single fault and considers it to be a community of fault fragments with an en-echelon arrangement. Which created a fault zone with an approximate width of 500 meters. Based on the evidence such as fault mirrors, fault steps, the direction of cutting of streams, and slickensides, he finds the direction of its longitudinal movement sinistral.

Suitable outcrops of carbonate gouges can be seen in the Astaneh region. This fault is seen as a fault zone. The existence of two fault lines parallel to each other and the creation of joints, fractures and deep cracks perpendicularly along the large faults and the operation of other large and small faults in the region due to tectonic forces have caused a faulted and sheared zone created.

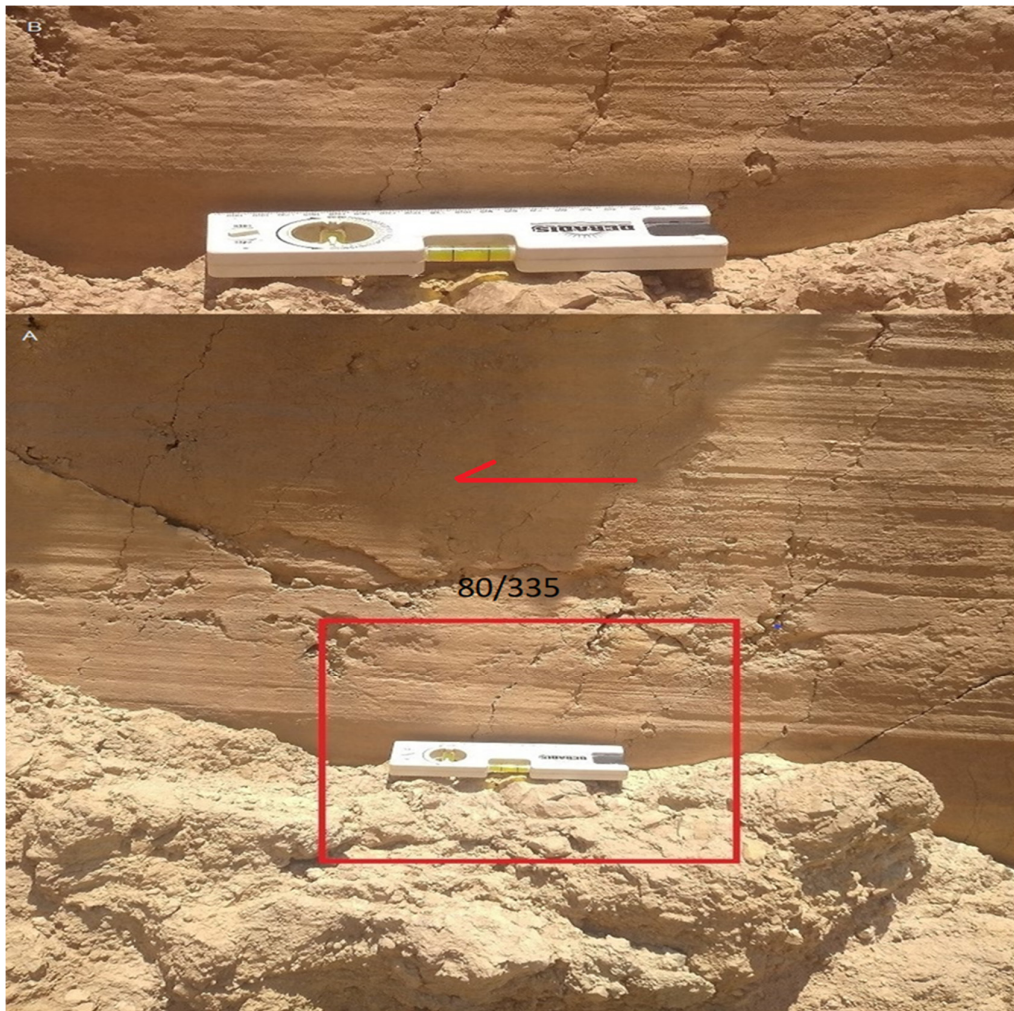


**Figure 3.** A north-facing view of fault surface with completely horizontal slickenside in carbonate rocks with dip and dip direction of this plane, where the red arrow shows the direction of movement of this block (hanging wall) and B, enlarged image of red box A. The location of this image is indicated by the black arrow in Figure 1

The co-occurrence of large and small pieces of limestone in this fault zone has resulted in a sharp increase in permeability. On the other hand, the presence of gouges has largely acted like a dam and caused directional currents. In any case, the mode of deformation in this fault remains transpressional and the crush zone is well developed in this fault, while the core of the fault is less developed.

The Astaneh Fault is known as an active and seismic fault in eastern Alborz (Nemati et al. 2012, Shokri et al. 2008, Hollingworth et al. 2010, Rizza et al. 2011). This fault features a fault zone with a variable width of 500 meters and significant shear in the waterways and Quaternary sediments. This fault with the characteristics mentioned and the specific seismic activity is a suitable place to study in particular the earthquake geology.

Based on the analysis of several tens of thousands of data from the Geophysics Institute Seismography center from 2000 to 2023 and the location of the related data by Google Earth, place of occurrence (the center) of thirty one events is located on the Astaneh fault and its branches. The magnitude of these events fluctuates from 3.5 to 4.7 MN. By scrutiny the catalog of earthquakes of the 20th century, 5 earthquakes were located on the Astaneh fault. These earthquakes have a magnitude from 4.5 to 5.8 (Ms and mb). The earthquake of March 5, 1935 is the largest of this series. Which occurred at the epicenter of 35.94 degrees latitude and 53.06

degrees longitude. After locating, it was determined that this earthquake is related in the Chashm fault (the western end of the Astaneh fault) and the activity of this fault. In any case, after locating the events, it is observed that the associated events are scattered almost along the entire length of the Astaneh fault and have an almost uniform distribution. The fact that the epicenters of earthquakes are spread along the entire length of the fault has a reason for the seismic activity of all parts of the Astaneh fault during less than two centuries. Table 1 shows the data of the events related to the Astaneh fault, and after placing these data in Google Earth, their image along with the Astaneh fault and their magnitude are shown in Figure 4.

**Table 1.** The data of earthquakes related to the Astaneh fault which columns of this table from left to right include row, date, time, latitude, longitude, magnitude and type of magnitude. The location of these data is shown in Figure 4

N.	Date	Time	Lat.	Long.	Mag.	M.Type	source
1	1935/03/05	10:26:00.0	35.940	53.060	5.8	M <sub>s</sub>	AMB
2	1982/02/05	23:37:12.0	36.120	53.671	4.5	m <sub>b</sub>	ISS
3	1986/03/26	15:18:09.20	36.010	53.670	4.6	m <sub>b</sub>	ISS
4	1995/11/23	19:29:34.0	36.000	53.431	4.2	mb	USGS
5	1997/11/03	06:59:31.1	36.331	54.452	4.5	M <sub>s</sub>	USGS
6	2002/06/28	19:27:30.0	36.311	54.068	4.3	MN	IRSC
7	2006/02/17	17:46:16.4	36.421	54.437	3.6	MN	IRSC
8	2006/11/13	15:00:29.3	36.339	54.096	4.1	MN	IRSC
9	2006/11/20	08:27:19.0	36.36	54.23	3.7	M <sub>s</sub>	IRSC
10	2006/12/20	05:00:36.2	36.186	53.836	4.2	MN	IRSC
11	2008/03/08	02:43:16.7	36.271	54.023	3.7	MN	IRSC
12	2012/08/05	19:54:43.7	36.085	53.726	3.6	MN	IRSC
13	2012/12/11	21:47:42.0	36.033	53.730	3.6	MN	IRSC
14	2013/01/10	05:16:53.0	36.014	53.566	3.7	MN	IRSC
15	2013/03/04	04:00:20.0	36.39	54.45	3.6	M <sub>s</sub>	IRSC
16	2014/07/09	02:52:09.0	36.390	54.112	3.5	M <sub>s</sub>	IRSC
17	2014/09/05	07:48:26.0	36.391	54.451	3.6	M <sub>s</sub>	IRSC
18	2015/03/02	06:53:54.6	36.285	54.139	3.9	MN	IRSC
19	2015/11/05	01:45:25.8	36.011	53.613	3.9	MN	IRSC
20	2016/05/24	15:32:56.0	36.332	54.187	4.1	MN	IRSC
21	2016/07/31	03:59:52.2	36.362	54.470	3.5	M <sub>s</sub>	IRSC
22	2016/12/31	04:59:52.2	36.377	54.456	3.5	MN	IRSC
23	2017/01/28	22:28:39.3	36.083	53.741	3.7	MN	IRSC
24	2017/06/22	02:00:18.3	36.187	53.919	4.6	MN	IRSC
25	2017/08/02	05:22:15.1	36.199	53.928	3.6	MN	IRSC
26	2018/03/20	02:40:21.0	35.94	53.39	4.4	MN	IRSC
27	2018/04/23	16:09:11.0	35.94	53.35	4.2	MN	IRSC
28	2018/09/12	05:02:27.0	35.92	53.26	3.5	MN	IRSC
29	2019/02/26	23:14:32.0	35.96	53.37	3.5	MN	IRSC
30	2019/07/04	06:27:32.0	36.136	53.980	4.7	MN	IRSC
31	2019/07/10	16:32:23.0	36.12	54.00	3.5	MN	IRSC
32	2019/11/22	20:06:48.0	35.95	53.31	4	MN	IRSC
33	2020/06/26	23:57:49.0	36.023	53.582	3.5	MN	IRSC
34	2020/11/21	05:42:18.0	36.361	54.512	4	MN	IRSC
35	2021/09/27	20:06:50.0	36.39	54.49	3.8	MN	IRSC
36	2022/03/18	16:17:08.0	36.011	53.582	4	MN	IRSC

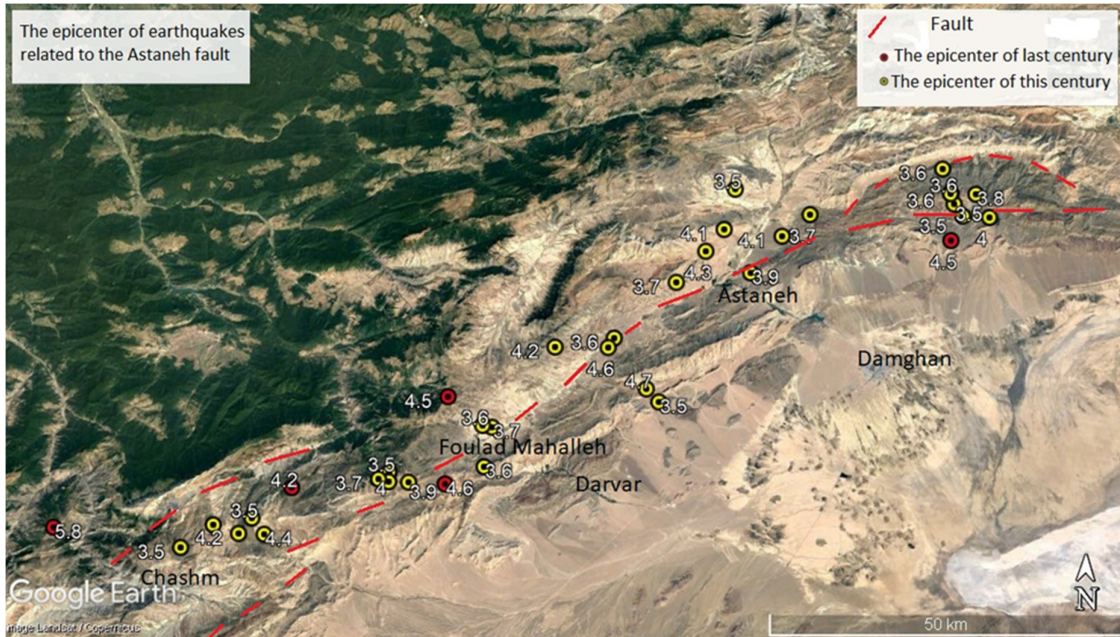


**Figure 4.** A view of the Astaneh fault in Google Earth and the epicenter of the earthquakes related to this fault. The red circles are the earthquakes of the last century and the yellow circles are the earthquakes of the current century. The magnitude events are listed next to them. The source of 5 earthquakes of the last century is AMB, ISS and USGS (red circles) and earthquakes of the current century is iscr (yellow circles)

#### **Description of the macroscopic condition of the Astaneh fault gouge:**

In the Astaneh Fault, there is both a damage zone and a fault core in some places. It should be noted that the gouges in the Astaneh fault are observed in discontinuous form and in the existing sites in a lenticular form. In some places where the core of the fault is not covered by Quaternary sediments and has a suitable outcrop, the gouge of the fault can be observed. In these places, in the middle of the lenses, there are fault gouges up to 35 cm thick, which gradually decrease in thickness towards the sides, and in some cases increase in thickness again, in other cases their outcrops disappear (Figure 5). Gouges fault is evident in all areas where the fault has intersected carbonate rocks, and at least one of the blocks on the sides of the fault should be carbonate rock. The gouge of the fault is very soft and varies in thickness (up to 35 cm) in different places. Due to the small particles of this type of rock, weathering has created very soft soil, and in most areas, the ground must be excavated to access the unweathered gouge. The gouge layers at these locations are almost sheet-shaped and the changes in material and fabric are quite evident due to the color changes (Figure 5). In the best outcrops where there are the thickest gouges, almost five layers can be seen. From the hanging wall side to the footwall side, these strata comprise a red gouge stratum immediately adjacent to the breccias and the surface of the hanging wall fault. Next to it, towards the footwall, there is a gray layer and then a yellow layer. After that, a gray layer and a yellow layer can be seen next to the breccia of the footwall (Figure 4). What is certain is that not all of these layers can be seen in all regions, but more or less some of them can be seen in most regions. The thickness of these layers is in most cases not equal and even in one outcrop this thickness increases and decreases. The thinnest of these layers is in most cases the red layer and the thickest of these layers is in most cases the yellow layer (Figure 5).

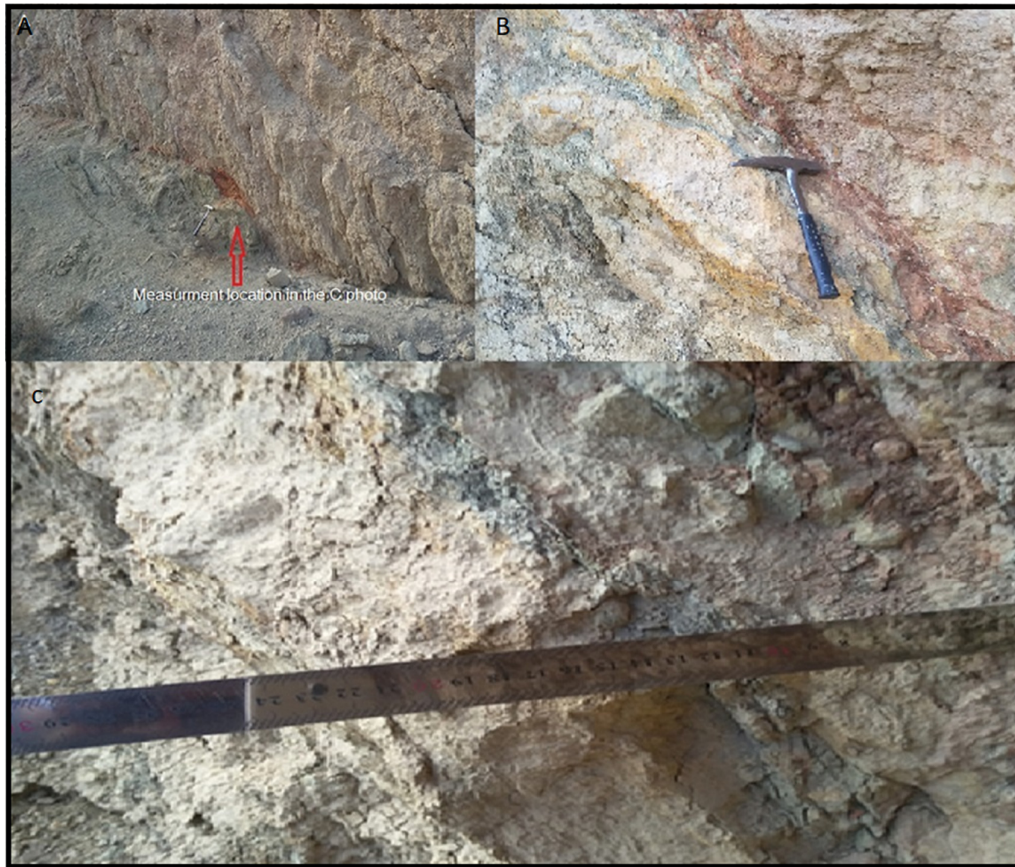


**Figure 5.** A view of the Astaneh Fault gouges north of the village of Astaneh. B is a close-up of image A, where the thin layer state of the gouge is clearly visible, and C is an image of the thickness of the gouge, indicated by the red arrow in Figure A

#### **Explanation of the mineralogical phases present in the Astaneh fault:**

To study the mineralogical composition of gouges, X-ray diffraction (XRD) was used in this study at Ferdowsi University Mashhad and Semnan University. XRD diffraction was performed based on the normal peak and without any special preparation of the clays. The dominant percentage of the phases in the samples of gouges were carbonates (calcium carbonate, dolomite, calcium oxide and magnesium oxide) depending on the protolith rock, which is carbonate. In addition, there are clay species (such as kaolinite, albite, sepiolite, montmorillonite, and antigorite), quartz, various iron oxides (such as siderite, goethite, and pure iron) and carbon (based on XRD analysis).

According to the results of XRD analysis, the total percentage of calcite and dolomite in the hanging wall protolith sample is more than 85%. Its phases are composed of carbonate rocks of Lar and Delichay formations consisting of calcite, dolomite, quartz, coesite and FeO. The noteworthy point is the absence of magnesium oxide and calcium oxide in the analysis results of this sample. The first sample of the fault gouge, was prepared of the first 6 centimeter (red layer) from the side of the hanging wall to the side of the foot wall. Kaolinite, polygorskite (attapulgite), goethite, quartz, halite, calcite, magnesium oxide, siderite and carbon phases were present in this sample. The next X-ray diffraction corresponds to the second 6.5 cm of the fault gouge in the same direction as the previous one (grey layer). In which there are mineral phases of dolomite, magnesium calcite, quartz, antigorite, periclase and calcium oxide or lime with the formula CaO. The third sample of this group was taken from the third 7 cm (yellow layer) of the fault gouge. This sample was prepared right from the center of the gouge fault, and the

number of phases in it is relatively higher than the other samples. In this sample, there are mineral phases of quartz, magnesium oxide and calcium oxide, montmorillonite, iron, carbon or graphite and salt. The next sample was prepared from the distance of 19.5 to 25 cm from the hanging wall side of the fault gouge (the gray layer of the second color). Antigorite, goethite, calcium oxide, sepiolite, quartz, montmorillonite and periclase phases are present in this sample. The next sample was prepared from a distance of 25 to 30 cm of the fault gouge from the side of the hanging wall to the footwall (the second yellow layer and the last layer of the fault gouge). The number of mineral phases that make up this sample is relatively high and it consists of quartz, carbon, albite, siderite, calcite, halite, magnesium oxide, goethite, montmorillonite and calcium oxide. The next sample in this category is prepared from the Shales of the Shemshak formation in footwall. In this sample, there are kaolinite, goethite, quartz, montmorillonite, antigorite and calcite mineral phases. The important point in this analysis is the absence of calcium oxide and magnesium oxide in the samples related to the protolith in the hanging wall and the footwall. These are two minerals or secondary phases that originate from calcite and dolomite due to heat. Both of these mineral phases exist in different layers of the fault gouge.

In these results, there is evidence of mineralogical changes that are related to the seismic slip of the fault. This evidence is the decarbonization of calcite and its transformation into calcium oxide (thermal decompose of calcite) and the decarbonization of dolomite and its transformation into periclase (Magnesium oxide). All these mineral changes, which are endothermic processes, point to their formation due to frictional heat caused by seismic slip. The dehydration of clays continues at temperatures between 400 and 600 degrees Celsius and the thermal decomposition of calcite occurs at temperatures between 750 and 950 degrees. The results indicate that during an earthquake, interactions between physicochemical processes such as calcite decarbonization and clay dehydration and similar thermal processes play an important role in facilitating earthquake slip.

The heat required for the thermal decomposition of carbonates and the dehydration of clays in the fault zone and fault cores is derived from the frictional heat of seismic slip. With this interpretation, it can be concluded that seismic slips must have occurred in the history of fault activity. Solutions in chemical reactions facilitate shape change, which is important in recrystallization. The action of solutions is to dissolve some minerals or to move and exchange some of their ionic components and finally to form new minerals or change the shape of minerals. In the fault zone, decarbonization and dehydration are again altered by the carbonization process and hydration. However, after careful examination of these stones, it was found that calcium oxide and magnesium oxide or periclase are present albeit in small amounts and their unchanged presence indicates thermal decomposition. In the fault gouges, the results of thermal decomposition and dehydration of the clays remain almost unchanged due to the fine grain size and lack of water penetration. Although the very fine grains of magnetite from siderite and periclase from dolomite are secondary and the result of thermal decomposition, they are stable and do not change over time. In each case, the presence of calcium oxide and magnesium oxide phases indicates the thermal decomposition of calcite and dolomite and is the result of frictional heat induced by seismic slipping. Figure 6 shows the plot of two XRD samples in which secondary phases of calcium oxide and magnesium oxide are present.

### **Description of the microstructure of the Astaneh Fault gouge**

In recent years, the scanning electron microscope SEM and the transmission electron microscope TEM have been used for microstructure analysis to examine more details and to detect very small grains in the fault zone.

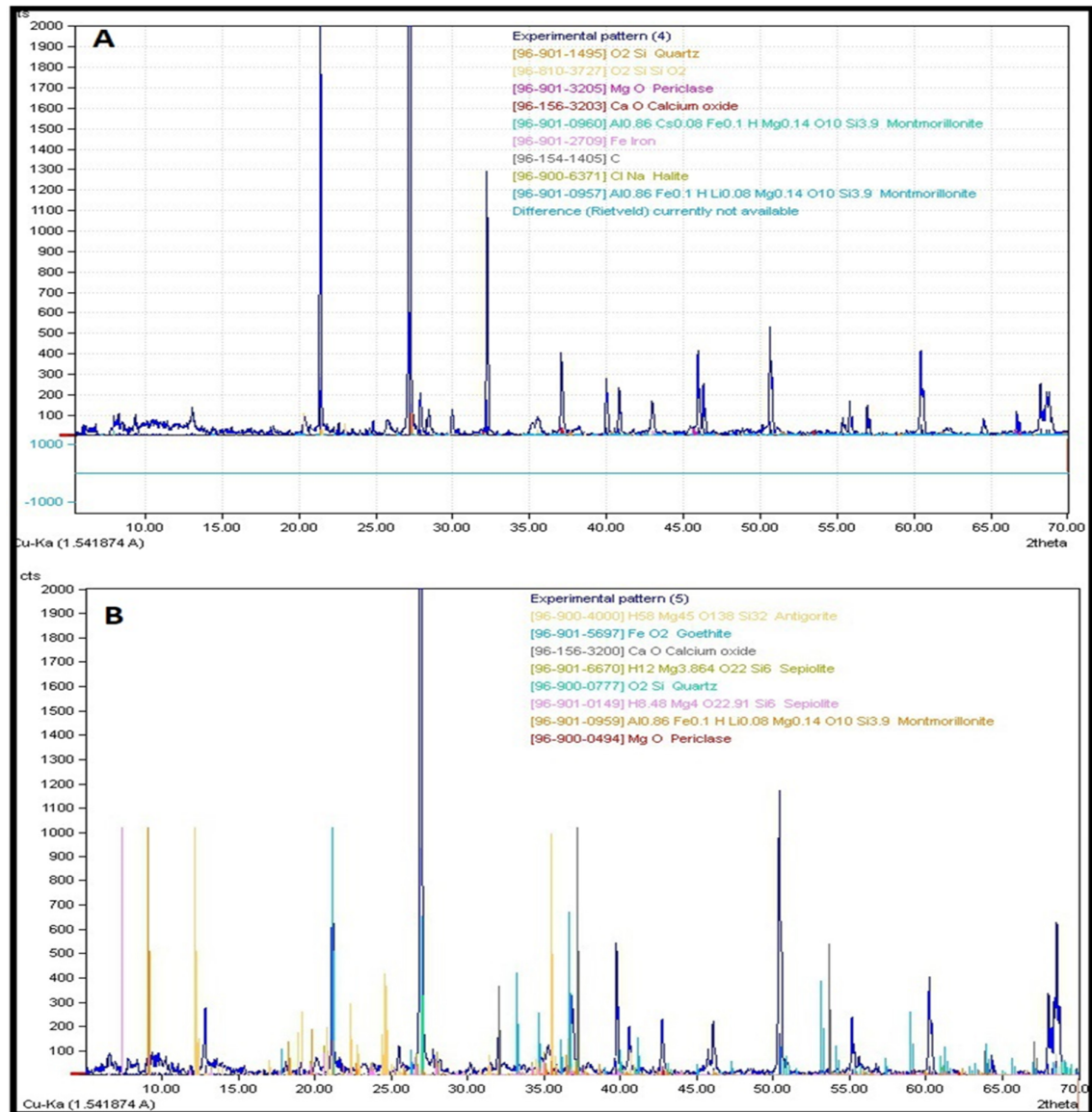


**Figure 6.** Two examples of diagrams for XRD analysis of the fault gouge. Picture A is from the third 5 cm and picture B is from the fourth 5 cm of the gouge. The phases in figure b include quartz, magnesium oxide (periclase), calcium oxide, montmorillonite, iron, carbon (graphite) and salt, in order of abundance. Phases in Figure B include antigorite, goethite, calcium oxide, sepiolite, quartz, montmorillonite and magnesium oxide (periclase)

This has led to significant progress in identifying microstructures, and there is a possibility that these microstructures may be useful indicators of frictional heating and seismic slip rates. For example, these microstructures can be named as stable products of thermal decomposition reactions in carbonates (Han et al. 2007) and circular accretion particles (Boullier et al., 2009; Boutareaud et al. 2008). Kim et al. 2003 suggested that the study of recrystallization by frictional heating in rock-forming minerals can occur at shallower depths.

However, no explicit relationship between the microstructures within the fault zone and the magnitude of seismic activity has been reported so far. But we will find a few concepts and consider cases from watching the gouge microstructures of dynamic issues and comparing them with exceedingly dynamic flaws with halfway surface cracks (Yanbao Li et al. 2022). In this study, we used scanning electrons SEM for microscopic study and analysis of the

micro fabric. For the investigation and study, samples of the existing gouge along the surface of the Astaneh fault were prepared. Over 3,000 images of different gouge samples from different locations were taken. This 3000 photos depends on the 500 samples that were prepared from each sample on average 6 photos. The method of preparing the samples was that as much as possible, sampling was done from all the points where the gouge fault protruded. In each place it was tried to sample all the available gouge layers. After viewing these images, the structures inside these images were carefully examined. The microstructures in these images can be identified into 4 different categories, including shear joints, calcite veins, welding of particles due to heat, and crushing of particles. Another thing is that the mentioned items are only available micro and nano structures. They are in a fault zone and not all of them are supposed to be used for seismic movement, and in this text we have also explained the examples of micro and nano structures observed in gouge particles and fault breccia that were able to be detected.

Briefly, the obvious signs of the Astaneh fault gouge are as follows: 1) The thickness of the fault gouge is not the same in all areas, and they are mostly seen as lenses with different lengths and widths, and thicknesses. 2) Under the microscope, only a very small number of samples show obvious micro-cracks in a conjugated form. But calcite veins are observed in a large number, which may be the result of carbonation of calcium oxide due to the penetration of water into the gouge. Or that they were originally formed as a result of chemical reactions. In any case, this sample of calcites denies the impermeability of gouges 100% and proves the penetration of water into them, although in a small amount. 3) Observed calcium oxide and thermal decomposition of dolomite and its conversion to periclase. These markers can provide useful evidence to identify microcracks in the surface and compensate for the limitations of traditional geological methods. Below is a description of each of these microstructures.

### *Shear joints*

In some images, nano- and micro-scale shear joints are observed. These joints are filled with secondary calcite in a large number of samples and in some others they just protrude as joints. Figure 7 shows an example of the typical shape of these joints, which can be seen in conjugate form with two different magnifications.

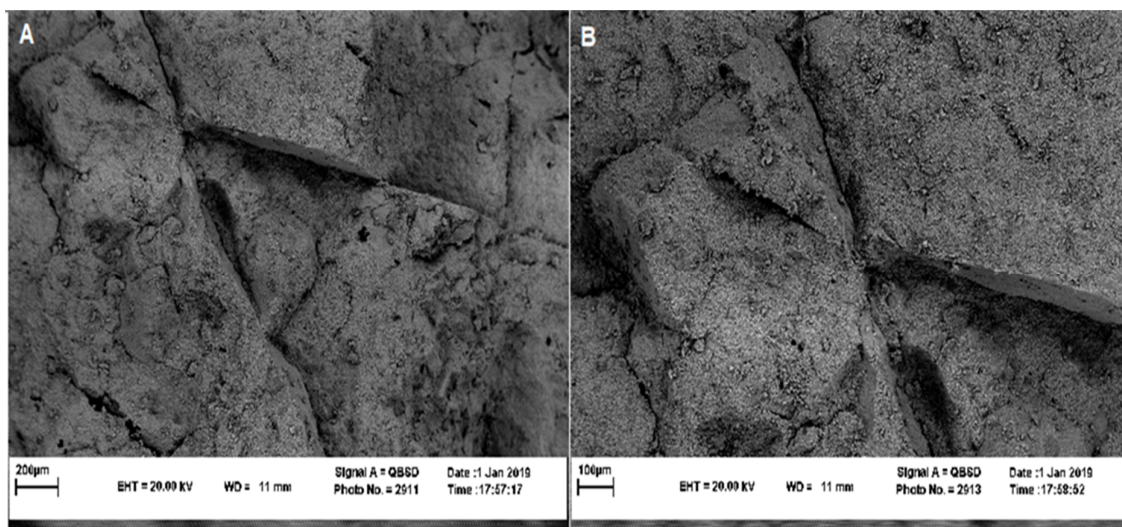


**Figure 7.** A is a view of a conjugate shear joint with 150x magnification and B is the same joint with 500x magnification

### *Calcite veins*

In geology, veins refer to separate crystalline plates in rocks. A vein forms when minerals carried by water and other solvents are deposited in the rock mass. Fluid flow is usually caused by hydrothermal circulation in the rock. The veins are younger than the surrounding rocks. What is important is that there is a possibility of a percentage of carbonate materials melting during the slip, and after the earthquake and seismic slip, the veins in the gouge grow and can be seen in different ways. It is possible that when slipping in some directions the amount of pressure and stress will be less than in others, and in these places, secondary materials resulting from slipping fusion have been placed.

In many images related to the Astaneh fault gouge, white calcite veins of different sizes and scales can be seen. In some other images, these veins are seen in conjugated form. Which is not particularly different from conjugate joints in position. Figure 8 shows an image of these veins. Two sources for these veins can be considered, one is deposition by hydrothermal solutions containing calcite in the empty space and the other is the combination of calcium oxide in the gouge with water and carbon dioxide and its conversion to calcite. Because the amount of porosity inside the gouge is very low, the origin of these veins from hydrothermal solutions is almost impossible. The presence of calcium oxide due to the thermal decomposition of calcite inside the gouge increases the possibility of formation from the second origin in these samples. These veins are seen in most samples and in different forms. There is no connection between these veins and the freeing sections of the shear zone. The releasing bend/step not detectable.

### *welding of particles due to heat*

In a large number of photos, we see the assembly of the particles and their joining together under the influence of heat and perhaps before the melting. This heat is definitely the result of frictional heat caused by seismic slips that can be seen in many images. Of course, this connection pattern exists in a large number of images. The important point is that the possibility of this deformation pattern formation occurs in the final crushing stages and because of the superheating in the final stages it is possible to form this welding and joining pattern. In Figure 9, images of this type of welding can be seen at different scales and magnifications.

Fine-grained calcite with a foam structure (fine bubbles) observed in the gouge layer probably indicates a welded gouge. Welded gouge grains can form under high pressure and low strain conditions with a single local slip during decomposition and shearing. A weld gouge with a bubble or foam structure in the fault zone where the wall rock does not show thermal metamorphic events, or a layer of plastic deformation immediately adjacent to the major shear zone of the cataclastic fault zone can be a signal of an earthquake fault (Han Ray et al. 2014).

### *Particle crushing*

Internal extension fracture is recognized as the main process occurring in the early stages of deformation. This process results in embryonic and intermediate cataclastic fabrics typical of shear zones. Shrinkage of grain due to the separation of pieces and subsequent shear failure is recognized as the main catalytic process operating at advanced strain stages, resulting in mature catalytic textures typical of gouge zones. This process should be considered the most important factor in changing the size of the gouge and breccia, varying in range and size up to the grain size. Figure 10 shows a picture of the crushing.

It should be noted that, apart from the mentioned cases, the deformation of minerals and their thermal decomposition can be seen in many pictures, which were shown in the previous sections as the result of XRD analysis to prove it. In addition, the thermal decomposition of calcite and

dolomite, as well as the dehydration of clays and the presence of carbon in the gouge can be used as a key to seismic slip (Kuo, 2011, Colletini et al 2013). Because there are no signs of metamorphism or igneous activity in the vicinity of this fault, it is certain that this structure was formed as a result of seismic slip.

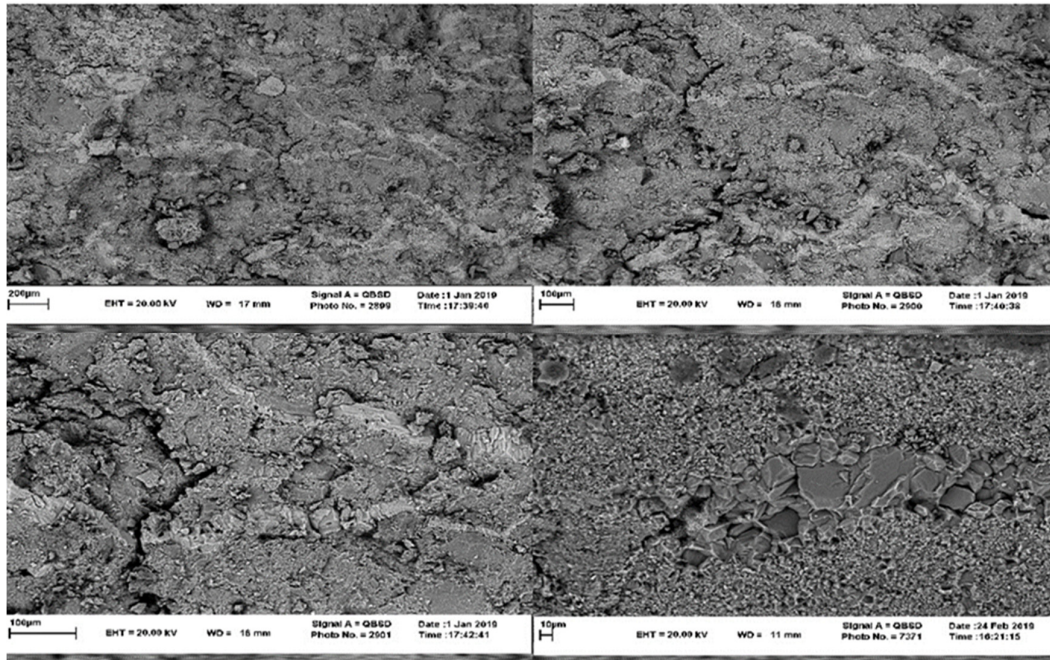


**Figure 8.** Four images of calcite veins with white color and different magnifications inside the Astaneh fault gouge

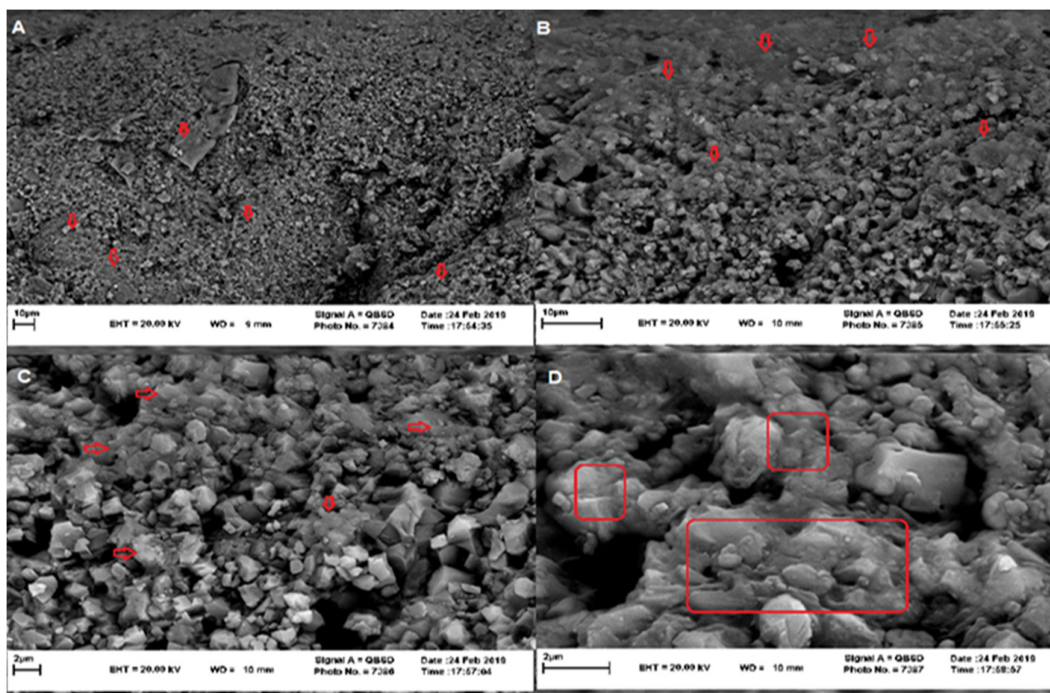


**Figure 9.** Images of Particle welding in different magnifications where the places of welding particles are shown with red arrows. A 1500x magnification B 4500x magnification C 10000x magnification and D 25000x magnification of image C. It should be noted that image D is the location of the vertical arrow in image C

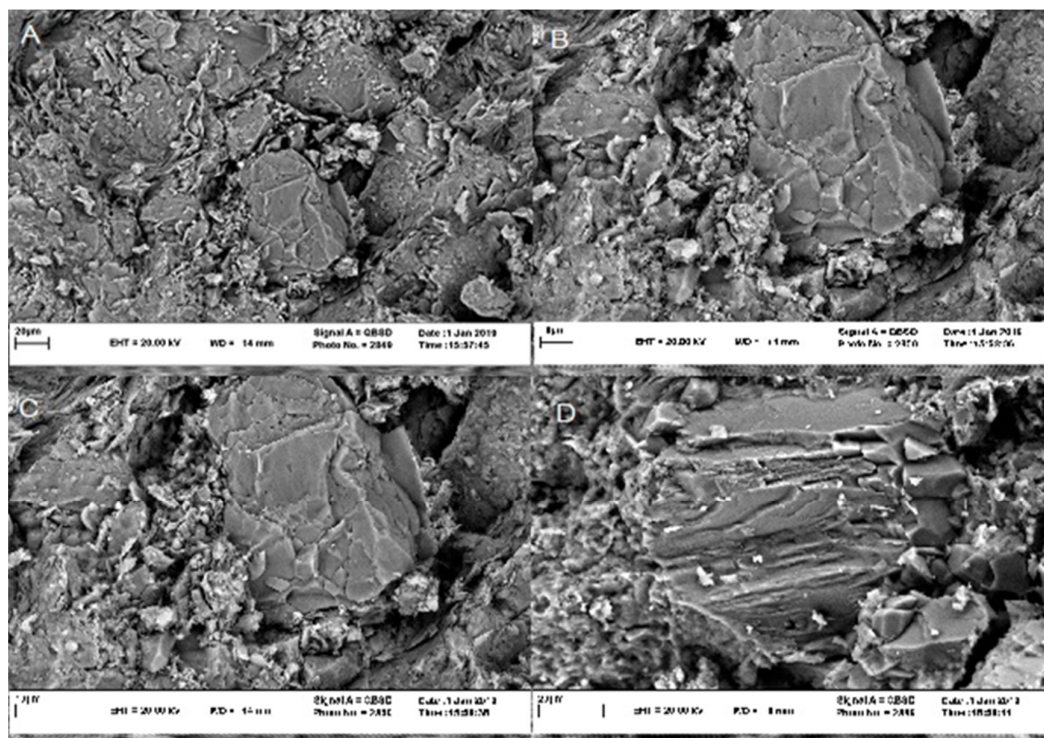


**Figure 10.** A is a view of crushing grains in the gouge with 2500 times magnification and B is an enlarged-twice image of A. C and D are other views of hair cracks in larger grains

## Conclusion

During faulting, many changes occur in rocks and minerals. These changes can be divided into the types of mineralogical changes, composition deformation, changes in rock structure and texture, and so on. Different types of these changes can be observed in the Astaneh fault zone. Example of mineralogical changes includes the thermal decomposition of calcite and dolomite and their conversion to calcium oxide and magnesium oxide (periclase). Both of these reactions are endothermic and require heat for conversion and progress. Due to the absence of igneous and metamorphism activity around this fault, the source of heat required for this change and mineral transformation is definitely the heat resulting from seismic slip. Structural changes can be observed in most of the faults and fault rocks, such as changes in size, porosity, permeability, cataclasticization, etc., and in all faults, this feature there is a significant difference between rock fault and host rock. Micro and nanostructure studies of fault gouge in Astaneh fault indicate that:

In terms of size, some structures are also observed in very small micro and nano sizes. According to the prepared images, it is possible to form conjugated shear joints in the micro and nano range, and if the conditions are right, it is possible to form this structure even in a micron-sized grain and particle. Apart from that, other constructions in the range of micro and nano can be mentioned calcite veins, welding of particles due to heat, and crushing of particles.

Rock crushing by shear and slip-in faults starts with large particles and moreover, it can be observed even at nano- and micro-sized particle sizes.

Many deformations, such as the fusion of particles and their uniformity in the final stage, are the result of an increase in frictional heat during seismic slips. A short-lived seismic slip causes high pressure and heat to act on the rock in the slip area, and in some areas even leads to rock melt, leading to the formation of pseudotachylite. But if the slipping temperature and pressure do not lead to melting then other changes in the rock will be caused. These changes, such as the stick and unification of particles together and the thermal decomposition of carbonate minerals,

can also be thought of as the result of seismic slip.

Some of the above definitely proves that the Astaneh fault is a seismic fault and seismic events (both historical and instrumental earthquakes) can definitely be attributed to it. Among the factors that can be used to demonstrate that a fault is seismic are the thermal decomposition of calcite and dolomite, welding of particles due to heat, the presence of a highly polished colored surfaces, etc. The presence of the above in the Astaneh fault indicates the occurrence of one or more earthquakes in this fault and is the key to confirming this issue. Therefore, it would be beneficial for future studies to explore alternative approaches, including the utilization of complementary data sources, advanced analytical techniques, and interdisciplinary collaborations. These endeavors can enhance our understanding of the timing and sequencing of distinct palaeoearthquakes.

## References

- Agosta, F., Prasad, M., Aydin, A., 2007. Physical properties of carbonate fault rocks, Fucino basin, central Italy: implications for fault seal in platform carbonates. *Journal of Geofluids*, 7: 19-32.
- Agosta, F., Kirschner, D.L., 2003. Fluid conduits in carbonate-hosted seismogenic normal faults of central Italy. *Journal of Geophysical Research*, 108, 2221. doi:10.1029/2002JB002013.
- Arzhannikova, A. V., Arzhannikov, S. G., Jolivet, M., Vassalo, R., Chauvet, A., 2011. Morphotectonic analysis of Pliocene-Quaternary deformations in the southeast of the Eastern Sayan, *Geotectonics*, 45: 142-156.
- Babaie, H.A., Hadizadeh, J., Babaei, A., 1995. Self-similar cataclasis in the Saltville thrust zone, Knoxville, Tennessee. *Journal of Geophysical Research*, 100: 18075- 18084.
- Barnhoorn, A., Bystricky, M., Burlini, L., Kunze, K., 2004. The role of recrystallization on the deformation behavior of calcite rocks: large strain torsion experiments on Carrara marble. *Journal of Structural Geology*, 26: 885-903.
- Billi, A., Di Toro, G., 2008. Fault-related carbonate rocks and earthquake indicators: recent advances and future trends. In: Landowe, S.J., Hammler, G.M. (Eds.), *Structural Geology: New Research*. Nova Science Publishers, Hauppauge, NY, USA, ISBN 978-1-60456-827-1.
- Bos, B., Peach, C.J., Spiers, C.J., 2000. Frictional-viscous flow of simulated fault gouge caused by the combined effects of phyllosilicates and pressure solution. *Journal of Tectonophysics* Volume 327, Issues 3-4: 173-194.
- Boutareaud, S., Calugaru, D.G., Han, R., Fabbri, O., Mizoguchi, K., Tsutsumi, A., Shimamoto, T., 2008. Clay-clast aggregates: A new textural evidence for seismic fault sliding? *Geophysical Research Letters Solid Earth*, Volume 35, Issue 5.
- Boullier, A-M., Yeh, E-C., Boutareaud, S., Song, S-R., Tsai, C-H., 2009. Microscale anatomy of the 1999 Chi-Chi earthquake fault zone. *Journal of Geochemistry Geophysics Geosystems*, 10(3): 1-25.
- Burkhard, M., 1993. Calcite-twins, their geometry, appearance and significance as stress-strain markers and indicators of stress regime: a review. *Journal of Structural Geology*, 15: 351-368.
- Caine, J. S., Evans, J. P., Forster, C. B., 1996. Fault zone architecture and permeability structure. *Geology*, 24: 1025-1028.
- Chester, F.M., Friedman, M., Logan, J.M., 1985. Foliated cataclases, *Tectonophysics*, 111: 139-146.
- Cladouhos, T.T., 1999. Shape preferred orientations of survivor grains in fault gouge. *Journal of Structural Geology*, 21, (4):419-436.
- Collettini, C., Viti, C., Tessei, T., Mollo, S., 2013. Thermal decomposition along natural carbonate faults during earthquakes. *Journal of Geology*, 41(8): 927-930.
- Collettini, C., Holsworth, R.E., Smith, S.A.F., 2009b. Fault zone structure and deformation processes along an exhumed low-angle normal fault. Implications for seismic behavior. In: Fukuyama, E. (Ed.), *Fault Zone Properties and Earthquake Rupture Dynamics*. International Geophysics Series, 94: 69-85.
- Collettini, C., Niemeijer, A., Viti, C., Marone, C. J., 2009a. Fault zone fabric and fault weakness. *Nature*, 462, 907-910.
- Holdsworth, R. E. 2004. Weak faults - Rotten cores. *Science*, 303: 181-182.
- Collettini, C. and Holdsworth, R. E., 2004. Fault zone weakening and character of slip along low-angle normal faults: insights from the Zuccale fault, Elba, Italy. *Journal of the Geological Society*. 161 (6): 1039-1052.

- Cowan, D.S., Cladouhos, T.T., Morgan, J.K., 2003. Structural geology and kinematic history of rocks formed along low-angle normal faults, Death Valley, California. *GSA Bulletin* (2003) 115 (10): 1230-1248.
- De Bresser, J.H.P., Spiers, C.J., 1993. Slip systems in calcite single crystals deformed at 300-800 C. *Journal of Geophysical Research*, 98: 6397-6409.
- Ferrill, D.A., Morris, A.P., 2008. Fault zone deformation controlled by carbonate mechanical stratigraphy, Balcones fault system, Texas. *AAPG Bulletin*, 92: 359-380.
- Ghisetti, F., Kirschner, D.L., Vezzani, L., Agosta, F., 2001. Stable isotope evidence for contrasting paleofluid circulation in thrust faults and normal faults of the central Apennines, Italy. *Journal of Geophysical Research*, 106: 8811-8826.
- Graham, B., Antonelli, M., Aydin, A., 2003. Formation and growth of normal faults in carbonates within a compressive environment. *Journal of Geology*, 31: 11-14.
- Hadizadeh, J., 1994. Interaction of cataclasis and pressure solution in a low temperature carbonate shear zone. *Pure and Applied Geophysics*, 143: 255-280.
- Han, R., Hirose, T., Shimamoto, T., 2010. Strong velocity weakening and powder lubrication of simulated carbonate faults at seismic slip rates. *Journal of Geophysical Research*, 115: 1-23.
- Han, R., Shimamoto, T., Ando, J., Ree, J., 2007a. Seismic slip record in carbonate bearing fault zones: an insight from high-velocity friction experiments on siderite gouge. *Journal of Geology*, 35: 1131-1134.
- Hayman, N. W., Housen, B.A., Cladouhos, T.T., Livi, K., 2004. Magnetic and clast fabrics as measurements of grain-scale processes within the Death Valley shallow crustal detachment faults. *JOURNAL OF GEOPHYSICAL RESEARCH*, 109, B05409, doi: 10.1029/2003JB002902, 2004.
- Hollingsworth, J., 2007- Active Tectonics of NE Iran, A dissertation submitted for the degree of Doctor of Philosophy at the University of Cambridge, (phd\_thesis).
- Hollingsworth, J., Nazari, H., Ritz, J. F., Salamati, R., Talebian, M., Bahroudi, A., Walker, R.T., Rizza, M., Jackson, J., 2010. Active tectonics of the east Alborz Mountains, NE Iran: Rupture of the left lateral Astaneh fault system during the great 856 A.D. Qumis earthquake. *Journal of Geophysical Research*, 115: 1-19. [https://geophysics.ut.ac.ir/Iranian\\_seismological\\_center\\_\(IRSC\)\\_HYPERLINK \"http://irsc.ut.ac.ir/\"irsc.ut.ac.ir](https://geophysics.ut.ac.ir/Iranian_seismological_center_(IRSC)_HYPERLINK\)
- Imber, J., Holdsworth, R. E., Butler, C. A., Strachan, R. A., 2001. A reappraisal of the Sibson Scholz fault zone model: The nature of the frictional to viscous ('brittle-ductile') transition along a longlived crustal-scale fault, Outer Hebrides, Scotland. *Tectonics*, 20: 601-624.
- Jackson, J., Priestley, K., Allen, M., Berberian, M., 2002. Active tectonics of the South Caspian Basin. *Geophysical Journal International*, 148: 214-245.
- Jefferies, S. P., Holdsworth, R. E., Shimamoto, T., Takagi, H., Lloyd, G. E., Spiers, C. J., 2006. Origin and mechanical significance of foliated cataclastic rocks in the cores of crustal-scale faults: examples from the Median Tectonic Line, Japan. *Journal of Geophysical Research-Solid Earth*, 111, B12303, doi: 10.1029/2005JB004205.
- Kennedy, L.A., Logan, J.M., 1997. The role of veining and dissolution in the evolution of fine-grained mylonites. *Journal of Structural Geology*, 19: 785-797.
- Kim, Y.S., Peacock, D.C.P., Sanderson, D.J., 2003. Mesoscale strike-slip faults and damage zones at Marsalforn, Gozo Island, Malta. *Journal of Structural Geology*, 25: 793-812.
- Knipe, R. J., 1989. Deformation mechanisms -recognition from natural tectonites. *Journal of Structural Geology*, 11: 127-146.
- Kuo, L-W., Song, S-R., Huang, L., Yeh, E-C., and Chen, H-F., 2011. Temperature estimates of coseismic heating in clay-rich fault gouges, the Chelungpu fault zones, Taiwan. *Journal of Tectonophysics* 502: 315-327.
- Liana-Funez, S., Rutter, E.H., 2005. Distribution of non-plane strain in experimental compression of short cylinders of Solnhofen limestone. *Journal of Structural Geology*, 27: 1205-1216.
- Moore, D. E., Rymer, M. J., 2007. Talc-bearing serpentinite and the creeping section of the San Andreas fault. *Nature*, 448: 795-797.
- Mortand, K., Woodcock, N.H., 2008. Quantifying fault breccia geometry: dent fault, NW England. *Journal of Structural Geology*, 30: 701-709.
- Micarelli, L., Benedicto, A., Wibberley, C.A.J., 2006. Structural evolution and permeability of normal fault zones in highly porous carbonate rocks. *Journal of Structural Geology*, 28: 1214-1227.
- Nazari, H., 2006. Analyse de la tectonique récente et active dans l'Alborz Central et la région de Téhéran: Approche morphotectonique et paleoseismologique. *Science de la terre et de l'eau*. Ph.D. thesis.

- University of Montpellier2, pp: 247 (in France).
- Nemati, M., Hatzfeld, D., Gheitanchi, M.R., Sadidkhouy, A., Mirzaei, N., and Moradi, A., 2012. Investigation of seismicity of the Astaneh Fault in the East Alborz. *Journal of Earth and Space Physics*, 37(2): 1-16.
- Newman, J., Mitra, G., 1994. Fluid-influenced deformation and recrystallization of dolomite at low temperatures along a natural fault zone, Mountain City window, Tennessee. *Geological Society of America Bulletin*, 106: 1267-1280.
- Pieri, M., Burlini, L., Kunze, K., Stretton, I., Olgaard, D.L., 2001a. Rheological and microstructural evolution of Carrara marble with high shear strain: results from high temperature torsion experiments. *Journal of Structural Geology*, 23: 1393-1413.
- Rahimi, B., 2002. Structural Study of Alborz Range in North Damghan, Ph.D. thesis. University of the shahid Beheshti, Iran, pp.232 (in Persian).
- Rizza, M., Mahan, S., Ritz, J-F., Nazari, H., Hollingsworth, J., Salamati, R., 2011. Using luminescence dating of coarse matrix material to estimate the slip rate of the Astaneh fault, Iran. *Quaternary Geochronology*, 6:390-406.
- Reinen, L. A., 2000. Seismic and Aseismic Slip Indicators in Serpentine Gouge. *Geology* 28 (2): 135-138.
- Salvini, F., Billi, A., Wise, D.U., 1999. Strike-slip fault-propagation cleavage in carbonate rocks: the Mattinata fault zone. *Journal of Structural Geology*, 21: 1731-1749.
- Scholz, C. H., 2002. *The Mechanics of Earthquakes and Faulting*. 2nd edn. Cambridge University Press, Cambridge.
- Shokri, M., Ghorashi, M., Nazari, H., Salamati, R., Talebian, M., Ritz, J.F., Mohammad khani, H., Shahpasand zadeh, M., 2008. Preliminary Results of Paleoseismologic Trenching along the Astaneh Fault. *Journal of Earth Sciences*, 18(number 70): 84-93 in Persian.
- Sibson, R. H., 1977. Fault rocks and fault mechanisms. *Journal of the Geological Society, London*, 133: 191-213.
- Smith, S.A.F., Di Toro, G., Kim, S., Ree, J-H., Nielsen, S., Billi, A., Spiess, R., 2013. Coseismic recrystallization during shallow earthquake slip. *Journal of Geology*, 41: 63-66.
- Smith, S.A.F., Colletini, C., Holdsworth, R.E., 2008. Recognizing the seismic cycle along ancient faults: CO<sub>2</sub>-induced fluidization of breccias in the footwall of a sealing low-angle normal fault. *Journal of Structural Geology*, 30: 1034-1046.
- Storti, F., Billi, A., Salvini, F., 2003. Particle size distributions in natural carbonate fault rocks: insights for non-self-similar cataclasis. *Earth and Planetary Science Letters*, 206: 173-186.
- Tullis, T. E., Burgmann, R. et al., 2007. Group report: rheology of fault rocks and their surroundings. In: Handy, M. R., Hirth, G. & Hovius, N. (eds) *Tectonic Faults: Agents of Change on a Dynamic Earth*. MIT Press, Cambridge, MA, 183-204.
- Tondi, E., 2007. Nucleation, development and petrophysical properties of faults in carbonate grainstones: evidence from the San Vito Lo Capo peninsula (Sicily, Italy). *Journal of Structural Geology*, 29: 614-628.
- Watts, L. M., Holdsworth, R. E., Sleight, J. A., Strachan, R. A., Smith, S. A. F., 2007. The movement history and fault rock evolution of a reactivated crustal-scale strike-slip fault: the Walls Boundary Fault Zone, Shetland. *Journal of the Geological Society, London*, 164: 1037-1058.
- Yanbao L., Lichun C., Yongkang R., Yuqiao C., 2022. Microscopic Characteristics of Fault Gouge in Minor-Surface-Rupture Faults: A Case Study in the Longmenshan Fault Zone, Eastern Tibetan ORIGINAL RESEARCH article *Front. Earth Sci. Structural Geology and Tectonics* Volume 10- 2022.
- Yuan, R., Zhang, B., Xu, X., Lin, C., 2013. Microstructural Features and Mineralogy of clay-rich Fault Gouge at the Northern Segment of the Yingxiu-Beichuan Fault, China. *Seismology Geol.* 35 (4): 685-700.
- Zhang, B., Lin, C., and Shi, L., 2002. Microstructural Features of Fault Gouges from Tianjing-Shan-Xiangshan Fault Zone and Their Geological Implications. *Sci. China Ser. D-earth Science*, 45 (1):72-80.

